Bioorganic & Medicinal Chemistry 17 (2009) 7542–7547

Contents lists available at ScienceDirect

Bioorganic & Medicinal Chemistry

journal homepage: www.elsevier.com/locate/bmc

Tedanol: A potent anti-inflammatory *ent*-pimarane diterpene from the Caribbean Sponge *Tedania ignis*

Valeria Costantino [a,*], Ernesto Fattorusso [a], Alfonso Mangoni [a], Cristina Perinu [a], Giuseppe Cirino [b], Luana De Gruttola [b], Fiorentina Roviezzo [b]

[a] Dipartimento di Chimica delle Sostanze Naturali, Università degli Studi di Napoli Federico II, via D. Montesano 49, 80131 Napoli, Italy
[b] Dipartimento di Farmacologia Sperimentale, Università degli Studi di Napoli Federico II, via D. Montesano 49, 80131 Napoli, Italy

ARTICLE INFO

Article history:
Received 29 June 2009
Revised 3 September 2009
Accepted 6 September 2009
Available online 13 September 2009

Keywords:
Diterpenes
Pimarane
Anti-inflammatory activity
COX-2 inhibitors
Marine sponges
Tedania ignis

ABSTRACT

Tedanol, a new brominated and sulfated pimarane diterpene was isolated from the Caribbean sponge *Tedania ignis*. Structure of tedanol was elucidated by mass spectroscopy and extensive NMR studies (including spectral simulation), and its absolute configuration was determined using the Mosher method. Tedanol showed a potent anti-inflammatory activity at 1 mg/kg evaluated in vivo in a mouse model of inflammation. After a single intraperitoneal administration, tedanol significantly reduced both the acute and the subchronic phases of carrageenan-induced inflammation. The anti-inflammatory activity was coupled with a strong inhibition of COX-2 expression, inhibition of cellular infiltration measured as mieloperoxidase (MPO) levels, and inhibition of iNOS expression. These features make tedanol a promising template for the development of new anti-inflammatory molecules with low gastrointestinal toxicity.

1. Introduction

Tedania ignis is a widespread Caribbean sponge, also known as 'fire sponge' because it causes a severe rash when handled by humans. Dermatites have also been reported to occur as a consequence of the contact with the sponge tissue.[1] It has not been determined so far which chemicals cause rash and dermatitis. Previous analyses of Caribbean samples of *T. ignis* led to the isolation of a new atisane derivative,[2] several diketopiperazines,[2,3] and some carbazole and carboline derivatives.[4] Many sponges contain a rich flora of symbiotic bacteria,[5] and *T. ignis* is one of these 'high-microbial-abundance sponges'. From a *Micrococcus* sp. obtained from the tissue of *T. ignis*, Cardellina et al. have isolated some of the diketopiperazines previously isolated from the sponge[6] along with four new benzothiazoles.[7]

Finally, in 1984 Schimtz's group reported the presence in *T. ignis* of tedanolide,[8] a potent cytotoxic macrolide that has been the target of intensive synthetic efforts. Although re-isolation of tedanolide was one of the reasons for our analysis of *T. ignis*, and in spite of our best efforts, we were not able to find any tedanolide in the extracts of the three different specimens of *T. ignis* from Bahamas that we examined.

However, our re-examination of the organic extract of *T. ignis* revealed the presence of tedanol (**1**), a new brominated and sulfated diterpene alcohol having an *ent*-pimarane skeleton. Tedanol showed a potent anti-inflammatory activity, evaluated as reduction of the carrageenan-induced mouse paw edema, coupled with a strong inhibition of COX-2 expression. In this paper, we report on the structure elucidation of tedanol and the study of its anti-inflammatory properties (Fig. 1).

2. Results

2.1. Isolation and structural elucidation

Samples of *T. ignis* collected in the mangroves of Sweeting Cay (Grand Bahama Island) during the 2007 Pawlik expedition were

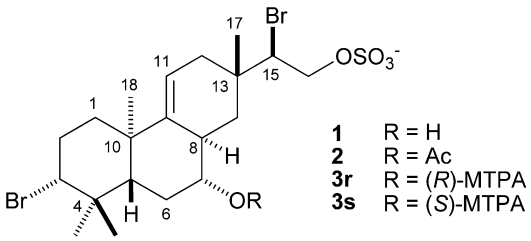

Figure 1. Structures of compounds **1**–**3**.

* Corresponding author. Tel.: +39 25081 678504; fax: +39 081 678552.
E-mail address: valeria.costantino@unina.it (V. Costantino).

0968-0896/$ - see front matter © 2009 Elsevier Ltd. All rights reserved.
doi:10.1016/j.bmc.2009.09.010

immediately chopped in small pieces and frozen, then shipped to our laboratory, where the samples were extracted in sequence with MeOH and $CHCl_3$. The MeOH extract was dried and partitioned between water and BuOH, and the combined BuOH and $CHCl_3$ extracts were subjected to reversed-phase column chromatography. The fraction eluted with H_2O/MeOH 2:8 showed to contain tedanol, but we were not able to obtain the compound in the pure form by HPLC only. Instead, pure tedanol (**1**) (6.5 mg) was obtained by reversed-phase HPLC, followed by preparative TLC using BuOH/AcOH/H_2O (60:15:25) as eluent.

The negative-ion ESI mass spectrum of **1** showed three M^- molecular ion peaks in the 1:2:1 ratio at *m/z* 545, 543, and 541, suggesting the presence of two bromine atoms in the molecule. A high-resolution measurement performed on the lowest-mass ion at *m/z* 541 determined the formula $C_{20}H_{31}Br_2O_5S$ (exp.: 541.0272, calcd for $C_{20}H_{31}{}^{79}Br_2O_5S$: 541.0258) for this ion.

A preliminary ^1H NMR analysis of compound **1** showed four methyl singlets between δ 1.13 and δ 1.01 indicatives of a polycyclic diterpene skeleton. The ^{13}C spectrum showed 20 carbon resonances, that were assigned with an HSQC experiment as four CH_3, six CH_2, six CH (one of which is sp^2, δ 115.9, and four linked to heteroatoms, δ 78.3, 70.8, 69.6, and 61.8), and four non-protonated carbon atoms (one of which is sp^2, δ 148.1). On the basis of the molecular formula and with the evidence of a double bond, it was clear that tedanol is a tricyclic diterpene.

The correlation peaks of the angular methyl groups [δ 1.06 (H_3-17), δ 1.13 (H_3-18), δ 1.01 (H_3-19), δ 1.08 (H_3-20)] in the HMBC spectrum allowed us to delineate two substructures (Fig. 2, bold bonds), which were connected thanks to the proton–proton vicinal couplings evidenced by the COSY spectrum (Fig. 2, solid bonds).

At this point, a pimarane skeleton was already delineated, except for the C-8/C-14 and C-8/C-9 bonds (Fig. 2, dashed bonds), connecting ring B with ring C. The bond between C-8 and C-9 was demonstrated by the allylic coupling between H-8 and H-11 and the homoallylic coupling between H-8 and H-12eq evidenced by the COSY spectrum. The coupling between H-8 and the two protons at C-14 could not be evinced from the COSY spectrum because the chemical shifts of H-8 and H-14eq were almost identical, leading to non-first-order multiplets. However, this couplings could be demonstrated by spectral simulation. The subspectrum of the 10-proton spin system comprising all protons on rings B and C was calculated, optimizing the unknown NMR parameters until the simulated multiplets reproduced accurately the experimental ones.

The results (Fig. 3) pointed to a 5.9 Hz coupling constant between H-8 and H-14eq and a 10.7 Hz coupling constant between H-8 and H-14ax, and also evidenced a quite large W coupling (3.1 Hz) between H-12eq and H-14eq. In addition, the bond between C-8 and C-14 bond was confirmed by the ROESY correlation peak between H-14ax (δ 1.37) and H-7 (δ 3.02).

The remaining atoms to be assigned from the molecular formula (two bromine, one sulfur, one hydrogen, and five oxygen atoms) pointed to the presence of one hydroxyl, one sulfate, and two bromide functions linked to the four deshielded carbon atoms C-3, C-7, C-15, and C-16. Derivatization of 0.6 mg of tedanol with Ac_2O in Py gave the monoacetyl derivative **2**, which showed a remarkable downfield shift of H-7 from δ 3.02 in the natural compound **1** to δ 4.39 in the acetate **2**, thus demonstrating that the hydroxyl function is located at position 7. The two bromine atoms present in the molecular formula were located at C-3 (δ 69.6) and C-15 (δ 61.8), because the chemical shift of these carbon atoms were about 15 ppm lower than those observed in pimaranes oxygenated at these positions,[9] while are close to those observed in a 3,15-dibromoisopimarane from *Laurencia perforata*.[13] Finally, the sulfate group was located at the remaining position 16, thus completing the planar structure of compound **1**.

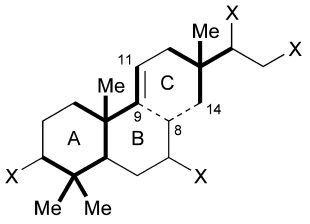

Figure 2. Elucidation of the pimarane skeleton of tedanol (**1**). Part structures determined from HMBC correlations of angular methyl protons are denoted with bold lines, and bond determined from COSY correlations are denoted with solid lines. X's represent heteroatoms.

2.2. Relative and absolute configuration

The relative configuration of the seven stereogenic centers of tedanol was assigned using coupling constant analysis combined with ROESY data. The A/B ring junction was established as *trans* because of the presence of a W long-range coupling between H-5 and H_3-18, indicative of their *anti* relationship. Relative configurations at C-3, C-7, and C-8 were established from the large vicinal coupling constants shown by H-3, H-7, and H-8 (see Table 1), indicating that they are all axial. This completed the relative stereochemistry of the *trans*-decaline moiety of the molecule (rings A and B). The ROESY correlation peaks of H-15 with H-8 and H_3-18, indicated that C-15 lies on the same side of the molecule as C-8 and C-18. This determined the relative configuration at C-13, and established that tedanol has the pimarane (or the enantiomeric *ent*-pimarane) skeleton.

The ROESY correlation peak between H-15 and H_3-18 was particularly interesting, because C-15 and C-18 are topologically far in the molecule. Analysis of a molecular model of tedanol easily demonstrated that H-15 and H_3-18 can be in close proximity to each other only if (a) the cyclohexene ring adopts the half-chair conformation such that C-15 is pseudo-axial and C-17 is pseudoequatorial and (b) the conformation around the C-13/C-15 bond is such that H-15 is directed inward of the cyclohexene ring (Fig. 4). The long-range W coupling between H-15 and H_3-17 observed in the COSY spectrum, indicative of their *anti* relationship, showed that this conformation around the C-13/C-15 bond is indeed largely predominant.

The torsional rigidity of the C-13/C-15 bond can be justified by unfavorable steric interactions of either the bromine atom or the $CH_2SO_3^-$ group with H-8 in the two alternative staggered conformations. More importantly, it was the key for the assignment of the relative configuration at C-15. In fact, the ROESY correlation peak between H-14eq and one of the protons at C-16 indicated that C-14 and C-16 are *gauche* oriented, and this, together with the *anti* relationship between H-15 and C-17, defined the relative configuration at C-15 as depicted in Figure 4.

As for the absolute configuration of tedanol, we used Mosher's method,[10] a reliable tool to establish the absolute configuration of secondary alcohols. Tedanol was allowed to react with (*S*)-(+)- and (*R*)-(−)-α-methoxy-α-trifluoromethylphenylacetyl chloride [(*S*)-(+)- and (*R*)-(−)-MTPA-Cl] to give, respectively, the 7-*O*-(*R*)-MTPA and 7-*O*-(*S*)-MTPA esters **3r** and **3s**, whose ^1H NMR spectra were acquired and assigned.

According to the Mosher model, the esters adopt a preferential conformation with the eclipsed CF_3 and C═O groups, and the phenyl group has a shielding effect on the neighboring protons. Thus, the observed $\Delta\delta$ values are consistent with the *R* configuration at C-7 (Fig. 5), and therefore indicate that tedanol has the *ent*-pimarane, and not the pimarane, skeleton.

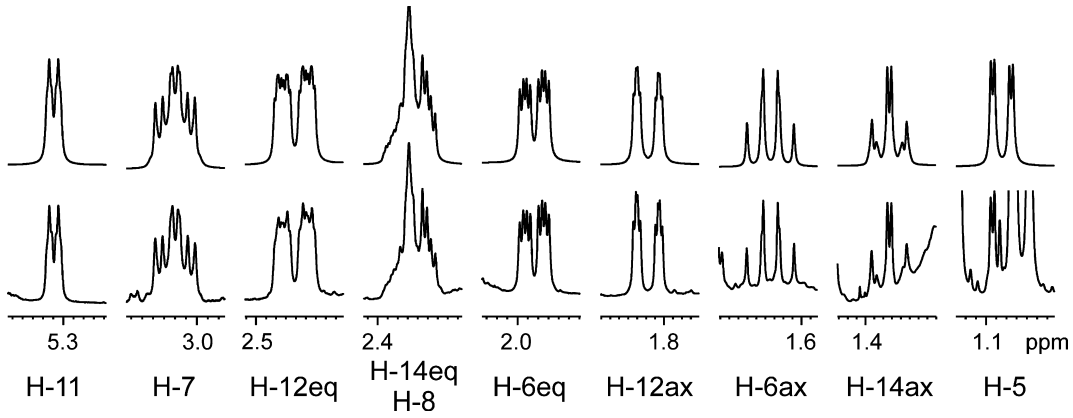

Figure 3. Simulated spectrum of the spin system of H-5 through H-14 (upper trace) compared to the experimental spectrum (lower trace). All the signals (including the non-first order multiplets of H8/H14eq and H-14ax) are accurately reproduced. Simulation parameters are: δ(H-5) 1.0846, δ(H-6ax) 1.6345, δ(H-6eq) 1.9834, δ(H-7) 3.0197, δ(H-8) 2.3699, δ(H-11) 5.3095, δ(H-12ax) 1.8184, δ(H-12eq) 2.4609, δ(H-14ax) 1.3731, δ(H-14eq) 2.3593, J(H-5/H-6ax) = 12.7 Hz, J(H-5/H-6eq) = 2.5 Hz, J(H-6ax/H-6eq) = −12.7 Hz, J(H-6ax/H-7) = 11.1 Hz, J(H-6eq/H-7) = 4.7 Hz, J(H-7/H-8) = 9.8 Hz, J(H-8/H-11) = 1.7 Hz, J(H-8/H-12ax) = 3.5 Hz, J(H-8/H-12eq) = 1.6 Hz, J(H-8/H-14ax) = 10.7 Hz, J(H-8/H-14eq) = 5.9 Hz, J(H-11/H-12ax) = 2.0 Hz, J(H-11/H-12eq) = 6.3 Hz, J(H-12ax/H-12eq) = −17.3 Hz, J(H-12eq/H-14eq) = 3.1 Hz, J(H-14ax/H-14eq) = −13.9 Hz.

Table 1
^{1}H and ^{13}C NMR data of tedanol **1** (CD_3OD)

Position		δ_H [mult., J (Hz)]	δ_C [mult.]
1	ax	1.55 (ddd, 13.5, 13.3, 3.6)	39.6 (CH_2)
	eq	1.70 (ddd, 13.3, 3.6, 3.4)	
2	ax	2.27 (dddd, 13.6, 13.5, 12.7, 3.4)	32.4 (CH_2)
	eq	2.16 (dddd, 13.6, 4.2, 3.6, 3.6)	
3		4.02 (dd, 12.7, 4.2)	69.6 (CH)
4		—	40.8 (C)
5		1.08 (dd, 12.7, 2.5)	51.6 (CH)
6	ax	1.62 (ddd, 12.7, 12.7, 11.1)	33.8 (CH_2)
	eq	1.98 (ddd, 12.7, 4.7, 2.5)	
7		3.02 (ddd, 11.2, 9.7, 4.7)	78.3 (CH)
8		2.37 (dddddd, 10.7, 9.8, 5.9, 3.5, 1.7, 1.6)[a]	40.3 (CH)
9		—	148.1 (C)
10		—	40.1 (C)
11		5.31(ddd, 6.3, 2.0, 1.7)	115.9 (CH)
12	ax	1.82 (ddd,17.3, 3.5, 2.0)	39.7 (CH_2)
	eq	2.46 (ddd, 17.3, 6.3, 3.1, 1.6)	
13		—	36.7 (C)
14	ax	1.37(dd, 13.9, 10.7)[a]	39.4 (CH_2)
	eq	2.36 (ddd, 13,9, 5.9, 3.1)[a]	
15		4.37 (dd, 8.9, 3.4)	61.8 (CH)
16	a	4.49 (dd,11.8, 3.4)	70.8 (CH_2)
	b	4.19 (dd, 11.8, 8.9)	
17		1.06 (s)	24.6 (CH_3)
18		1.13 (s)	21.7 (CH_3)
19		1.01 (s)	18.7 (CH_3)
20		1.08 (s)	30.9 (CH_3)

[a] Non-first-order multiplet, coupling constants determined by spectral simulation (see text and Fig. 3).

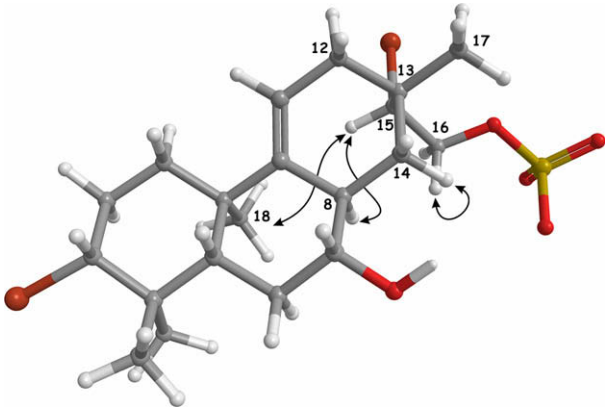

Figure 4. ROESY correlations used to determine relative configurations at C-13 and C-15.

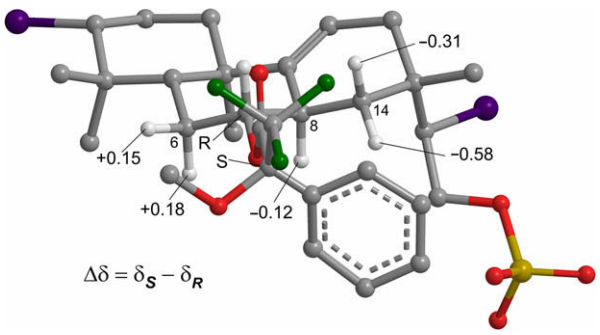

Figure 5. Preferred conformation of the (*S*)-MTPA ester of tedanol (**3s**) according to the Mosher model, and observed $\Delta\delta$ of the neighboring protons.

2.3. Anti-inflammatory activity

The anti-inflammatory activity was evaluated as inhibition of the carrageenan-induced paw edema in mice.[11,12] Intraperitoneal administration of tedanol (0.1–1 mg/kg) to mice 30 min before subplanatar carrageenan injection, causes a significant and dose related reduction in edema (Fig. 6). Because edema evaluation gives information relative to inflammatory swelling, due to vascular leakage, but not on cell infiltration, mieloperoxidase (MPO) levels were also measured. MPO evaluation is a widely used indirect index of cell infiltration. The systemic administration of tedanol prior to induction of inflammation (1 mg/kg) significantly inhibits MPO activity at 4 and 48 h after carrageenan injection (Fig. 7).

In order to further investigate on the mechanism underlying tedanol anti-inflammatory activity, western blot analysis was performed on the paws harvested from mice pretreated with tedanol at the highest dose. Tedanol (1 mg/kg) significantly inhibited COX-2 expression both in the early phase (2 and 4 h) and in the second edema phase (48 and 72 h). Conversely, tedanol did not affect COX-1 expression in the early phase, but significantly inhibited its expression in the second phase. Tedanol pretreatment significantly inhibited iNOS expression at 2 h and 48 h only (Fig. 8). These data suggest that tedanol exerts its anti-inflammatory activity by reducing both vascular permeability and cell migration that involves

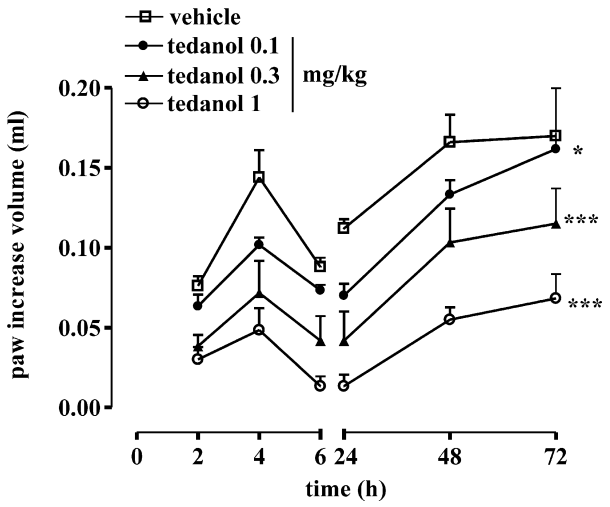

Figure 6. Effect of systemic administration of tedanol (0.1–1 mg/kg) on carrageenan-induced mouse paw edema (* p <0.05; *** p <0.001 vs vehicle).

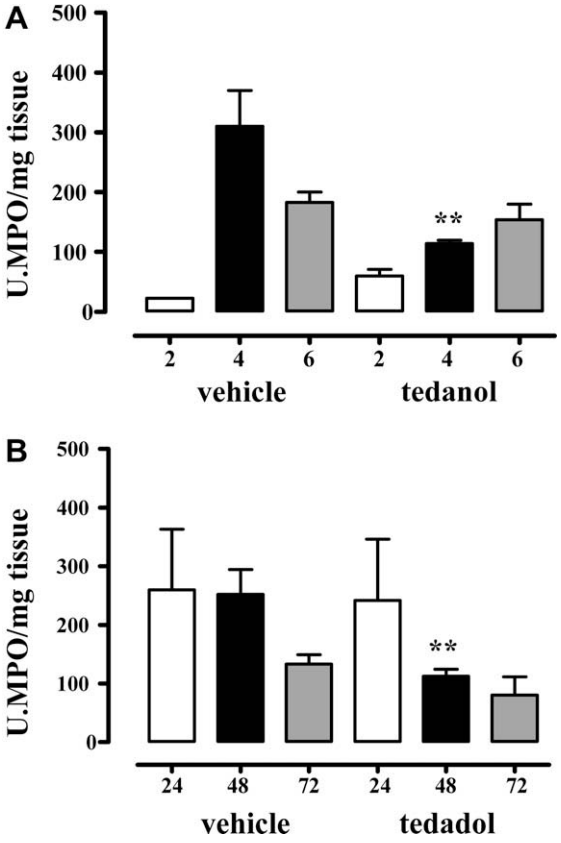

Figure 7. MPO evaluation performed on inflamed mouse paws harvested from mice systemically treated with the higher dose of tedanol (1 mg/kg)- versus vehicle-treated mice in the first (panel A) and second phase (panel B) of edema (** p <0.01 vs vehicle).

mainly modulation of expression of COX-2 and, to a lesser extent, of COX-1 and iNOS.

3. Discussion

The structure of the new diterpene tedanol from *T. ignis* was established as the brominated and sulfated *ent*-pimarane diterpene

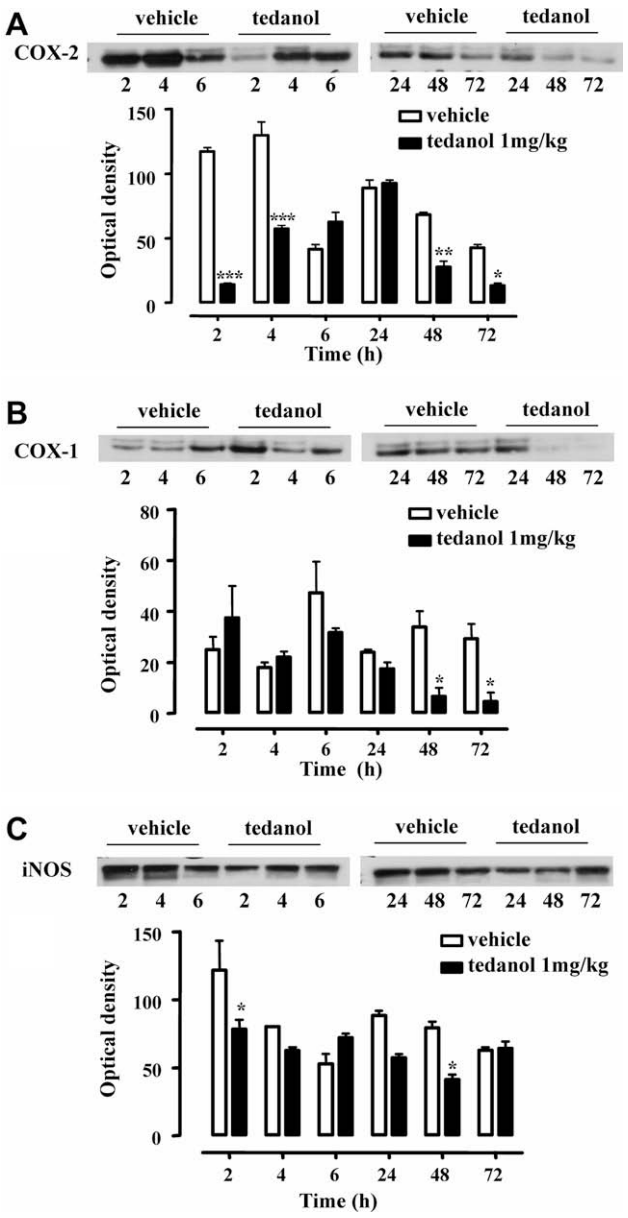

Figure 8. Western blot analysis for COX-2 (panel A), COX-1 (panel B) and iNOS (panel C) performed on inflamed mouse paws harvested from tedanol- (1 mg/kg) or vehicle-treated mice. The blots are representative of three different experiments reported as densitometry analysis in bar graphs (* p <0.05; ** p <0.01; *** p <0.001 vs vehicle).

alcohol **1**. To the best of our knowledge this is the first report of an *ent*-pimarane diterpene from a sponge tissue. The known natural metabolites most closely related to tedanol are a dibromoditerpene isolated in 1984 from the alga *L. perforata*[13] and its diacetate from the sponge *Spongia zymocca*,[14] but these are compounds based on an isopimarane rather than an *ent*-pimarane skeleton.[15]

Tedanol turned out to be biologically attractive because it showed a potent anti-inflammatory activity, evaluated as reduction of the carrageenan-induced mouse paw edema. Another diterpene with the pimarane skeleton, acanthoic acid,[16] which is present in the Korean plant *Acanthopanax koreanum* traditionally used in popular medicine for the cure of rheumatism, has been shown to possess in vitro COX-2 inhibitory activity.[17,18] However, no data are available to date on the in vivo anti-inflammatory activity of this compound or other natural pimarane diterpenes. Indeed, in vivo anti-inflammatory activity requires, in addition to COX-2 inhibition, a favorable pharmacokinetic profile and lack of toxicity.

In the present study, we demonstrated that tedanol does possess in vivo anti-inflammatory activity. After a single intraperitoneal administration, tedanol significantly reduced both the acute (4 h) and subchronic (48 h) phase of the carrageenan-induced paw edema in mice. The anti-inflammatory activity was coupled with a strong inhibition of COX-2 expression, inhibition of cellular infiltration measured as mieloperoxidase (MPO) levels, and inhibition of iNOS expression. These features, together with its solubility in water, not frequently encountered among natural diterpenes, make tedanol a promising template for the development of new anti-inflammatory molecules with low gastrointestinal toxicity.

4. Experimental section

4.1. General experimental procedures

High-resolution ESI-MS spectra were performed on a Bruker APEX II FT-ICR mass spectrometer. ESI MS experiments were performed on a Applied Biosystem API 2000 triple-quadrupole mass spectrometer. The spectra were recorded by infusion into the ESI source using MeOH as the solvent. Optical rotations were measured at 589 nm on a Perkin–Elmer 192 polarimeter using a 10-cm microcell. ^{1}H and ^{13}C NMR spectra were determined on Varian UnityInova spectrometers at 500 and 700 MHz; chemical shifts were referenced to the residual solvent signal (CD_3OD: $\delta_H = 3.31$, $\delta_C = 49.0$). For an accurate measurement of the coupling constants, the one-dimensional ^{1}H NMR spectra were transformed at 128 K points (digital resolution: 0.05 Hz). Homonuclear ^{1}H connectivities were determined by COSY experiments. Through-space ^{1}H connectivities were evidenced using a ROESY experiment with a mixing time of 450 ms. The reverse single-quantum heteronuclear correlation (HSQC) spectra were optimized for an average $^1J_{CH}$ of 145 Hz. The multiple-bond heteronuclear correlation (HMBC) experiments were optimized for a $^3J_{CH}$ of 8 Hz. Spectral simulations were performed using Bruker's NMRSIM program. High performance liquid chromatographies (HPLC) were achieved on a Varian Prostar 210 apparatus equipped with an Varian 350 refractive index detector.

4.2. Collection, extraction, and isolation

Specimens of *T. ignis* were collected in the Mangroves of Sweeting Cay (Grand Bahama Island) during the 2007 Pawlik expedition. They were frozen immediately after collection and kept frozen until extraction. The sponge (58 g of dry weight after extraction) was homogenized and extracted with MeOH (5 × 1 L) and then with $CHCl_3$ (2 × 1 L). The MeOH extracts were partitioned between H_2O and *n*-BuOH, and the BuOH layer was combined with the $CHCl_3$ extract and concentrated in vacuo. The organic extract (12.8 g) was chromatographed on a column packed with RP-18 silica gel. A fraction eluted with MeOH/H_2O 8:2 (195 mg) was subjected to HPLC separation on an RP-18 column [MeOH/H_2O (7:3)], thus affording a fraction (6.5 mg) mainly composed of compound **1**. Final purification was achieved by preparative TLC (SiO_2, 20 × 20 cm, 0.5 mm thick) using BuOH/AcOH/H_2O (60:15:25) as eluent, which gave 3.1 mg of pure tedanol **1**.

4.2.1. Tedanol (1)

Colorless amorphous solid, $[\alpha]_D^{25} = +6$ (*c* 0.1 in MeOH); HRESIMS (negative ion mode, MeOH) 541.0272 (M^-, $C_{20}H_{31}{}^{79}Br^{81}BrO_5S$ gives 541.0258); ESIMS (negative ion mode, MeOH) *m/z* 543, 541, and 539 (M^-); ^{1}H and ^{13}C NMR: Table 1.

4.2.2. Tedanol 7-*O*-acetate (2)

Tedanol **1** (0.6 mg) was dissolved in 500 μl of pyridine and 500 μl of acetic anhydride were added. The reaction was allowed to proceed for 18 h at room temperature, and the reaction mixture was then dried under vacuum, giving 0.6 mg of tedanol 7-*O*-acetate (**2**): colorless amorphous solid; ^{1}H NMR (CD_3OD): δ 5.39 (1H, br d, *J* = 6.3 Hz, H-11), 4.45 (1H, dd, *J* = 11.6 and 4.1 Hz, H-16a), 4.39 (1H, ddd, *J* = 10.8, 10.6, and 4.7 Hz, H-7), 4.36 (1H, dd, *J* = 8.2 and 4.1 Hz, -H-15), 4.20 (1H, dd, *J* = 11.6 and 8.2 Hz, H-16b), 4.04 (1H, dd, *J* = 12.7 and 4.2 Hz, H-3), 2.66 (1H, m, H-8), 2.46 (1H, br d, *J* = 17.4 Hz, H-12eq), 2.29 (1H, m, H-2ax), 2.17 (2H, overlapped, H-2ax and H-14eq) , 2.03 (1H, ddd, *J* = 12.5, 4.6, and 2.5 Hz, H-6eq), 1.84 (1H, ddd, *J* = 17.4, 3.5, and 2.2 Hz, H-12ax), 1.72 (2H, overlapped, H-1eq and H-6ax), 1.58 (1H, ddd, 13.3, 13.4, and 3.6 Hz, H1ax), 1.31 (1H, m, H-14ax), 1.160 (3H, s, H_3-18), 1.16 (1H, dd, *J* = 12.8 and 2.5 Hz, H-5), 1.055 (3H, s, H_3-20), 1.046 (3H, s, H_3-17), 0.998 (3H, s, H_3-19).

4.3. MTPA derivatization of tedanol

Tedanol (0.4 mg) was dissolved in 500 μl of pyridine, and (*S*)-(+)-MTPA chloride (10 μl) was added. The reaction was allowed to proceed for 18 h at room temperature, and the reaction mixture was then dried under vacuum, giving, the 7-*O*-(*R*)-MTPA ester **3r**. The same procedure, using (*R*)-(−)-MTPA chloride, gave the 7-*O*-(*S*)-MTPA ester **3s**.

4.3.1. Tedanol 7-*O*-(*R*)-MTPA ester (3r)

Colorless solid; ^{1}H NMR (CD_3OD): δ 5.42 (1H, br d, *J* = 6.3 Hz, H-11), 4.62 (1H, ddd, *J* = 10.9, 10.9, and 4.7 Hz, H-7), 4.36 (1H, dd, *J* = 11.6 and 3.1 Hz, H-16a), 4.33 (1H, dd, *J* = 9.0 and 3.1 Hz, H-15), 4.11 (1H, dd, *J* = 11.6 and 9.0 Hz, H-16b), 4.05 (1H, dd, *J* = 12.6 and 4.2 Hz, H-3), 2.70 (1H, m, H-8), 2.47 (1H, br d, *J* = 17.4 Hz, H-12eq), 2.26 (1H, dddd, *J* = 13.3, 13.3, 13.3, and 3.2 Hz, H-2ax), 2.17 (1H, dddd, *J* = 13.7, 3.9, 3.9, and 3.9 Hz, H-2eq), 2.01 (1H, ddd, *J* = 12.1, 4.6, and 2.4 Hz, H-6eq), 1.95 (1H, ddd, *J* = 13.8, 5.9, and 3.1 Hz, H-14eq), 1.85 (1H, ddd, *J* = 17.4, 3.1, and 2.4 Hz, H-12ax), 1.71 (1H, ddd, *J* = 13.4, 3.4, and 3.4 Hz, H-1eq), 1.62 (quartet, *J* = 12.2 Hz, H-6ax), 1.59 (1H, m, H-1ax) , 1.34 (1H, *J* = 13.8 and 10.7 Hz, H-14ax), 1.20 (1H, dd, *J* = 12.7 and 2.3 Hz, H-5), 1.11 (3H, s, H_3-18), 1.06 (3H, s, H_3-20), 1.00 (3H, s, H_3-17), 0.94 (3H, s, H_3-19).

4.3.2. Tedanol 7-*O*-(*S*)-MTPA ester (3s)

Colorless solid; ^{1}H NMR (CD_3OD): δ 5.37 (1H, br d, *J* = 6.3 Hz, H-11), 4.52 (1H, ddd, *J* = 10.9, 10.9, and 4.7 Hz, H-7), 4.22 (1H, dd, *J* = 9.8 and 2.7 Hz, H-15), 4.04 (2H, overlapped, H-3 and H-16a), 3.88 (1H, dd, *J* = 11.9 and 9.8 Hz, H-16b), 2.57 (1H, m, H-8), 2.42 (1H, br d, *J* = 17.4 Hz, H-12eq), 2.27 (1H, dddd, *J* = 13.3, 13.3, 13.3, and 3.2 Hz, H-2ax), 2.17 (2H, overlapped, H-2eq and H-6eq), 1.80 (1H, quartet, *J* = 12.1 Hz, H-6ax), 1.77 (1H, ddd, *J* = 17.4, 3.3, and 2.4 Hz, H-12ax), 1.70 (1H, ddd, *J* = 13.4, 3.4, and 3.4 Hz, H-1eq), 1.57 (1H, ddd, *J* = 13.4, 13.4, and 3.5 Hz, H-1ax) , 1.37 (1H, m, H-14eq), 1.21 (1H, dd, *J* = 12.7 and 2.4 Hz, H-5), 1.13 (3H, s, H_3-18), 1.09 (3H, s, H_3-20), 1.03 (1H, *J* = 13.9 and 10.9 Hz, H-14ax), 1.00 (3H, s, H_3-19), 0.85 (3H, s, H_3-17).

4.4. Mouse paw edema

Male CD-1 mice weighing 23–27 g were separated in groups (*n* = 6) and lightly anesthetized with enflurane. Each group of animals received subplantar injection of 50 μl of carrageenan 1% w/v.[11,12] Paw volume was measured using a hydroplethismometer specially modified for small volumes (Ugo Basile, Milan, Italy) immediately before the subplantar injection and 2, 4,6, 24, 48, or 72 h thereafter. The increase in paw volume was evaluated as difference between the paw volume at each time point and the basal paw volume. In another set of experiments, CD-1 were subjected to a previous intraperitoneal injection of tedanol **1** (200 μl of water

solution, 0.1–1 mg/kg), and after 30 min each group of animals received subplantar injection of 50 μl of carrageenan. Data are expressed as mean ± SEM. The level of statistical significance was determined by two-way analysis of variance (ANOVA) followed by Bonferroni's test for multiple comparisons, using the GraphPad Prism software.

4.5. Western blot

Carragenan-injected paws from CD-1 mice sacrificed at 2, 4, 6 24, 48, and 72 h were homogenised in a 10 mM HEPES pH 7.4 buffer containing saccharose (0.32 M), EDTA (100 μM), dithiothreitol (1 mM), phenylmethylsulfonyl fluoride (1 mg/ml), and leupeptin (10 μg/ml)[11] using a Polytron homogenizer (3 cycles of 10 s at maximum speed). After centrifugation at 3000 rpm for 15 min, protein supernatant content was measured by Bradford reagent, and protein concentration was adjust at 30 μg. Protein samples were loaded on 10% PAGE–SDS and transferred onto nitrocellulose membranes for 45 min at 250 mA. Membranes were blocked in PBS-Tween 20 (0.1%) containing 5% non-fat milk and 0.1% BSA for 30 min at 4 °C. Membranes were washed with PBS-Tween 20 (0.1%) at 5 min intervals for 30 min, and incubated with anti-COX-1, anti-COX-2, anti-iNOS, and anti-eNOS overnight at 4 °C. Blots were washed with PBS-Tween 20 (0.1%) at 5 min intervals for 30 min and incubated with HRP-anti-rabbit IgG (1:20,000) for 2 h at 4 °C. The immunoreactive bands were visualized using an enhanced chemiluminiscence system (ECL; Amersham, USA).

4.6. MPO measurement

Mice from different groups were sacrificed with CO_2 at 2, 4, 6 24, 48, and 72 h after carrageenan injection. Injected paws were cut, weighted and homogenated in 1 ml of HTAB buffer using a Polytron homogenizer (2 cycles of 10 s at maximum speed). After centrifugation of homogenates at 10,000 rpm for 2 min, supernatant fractions were assayed for MPO activity using the method described by Bradley et al.[19] Briefly, samples were mixed with phosphate buffer containing 1 mM *O*-dianisidine dihydrochloride and 0.001% hydrogen peroxide in a microtiter plate reader. Absorbance was measured at 450 nm taking three reading at 30 s intervals. Units of MPO were calculated considering that 1 U. MPO = 1 μmol H_2O_2 split , and 1 μmol H_2O_2 gives a change in absorbance of 1.13×10^{-2} nm/min.

Acknowledgments

This research work was supported by MIUR PRIN 2007 (Grant no. 2007KZ9W5J) and by the European Project NatPharma (Grant agreement no. 229893). A warm thank you is due to Professor J. R. Pawlik, University of North Carolina at Wilmington, for inviting them to participate to the '2007 Pawlik Expedition' under the National Science Foundation project grant entitled 'Assessing the chemical defenses of Caribbean Invertebrates', during which the material was collected, and Prof. Sven Zea (Universidad Nacional de Colombia) for identifying the sponge. Mass and NMR spectra were recorded at the 'Centro di Servizi Interdipartimentale di Analisi Strumentale', Università di Napoli 'Federico II'. The assistance of the staff is gratefully acknowledged.

Supplementary data

Supplementary data associated with this article can be found, in the online version, at doi:10.1016/j.bmc.2009.09.010.

References and notes

1. Yaffee, H. S.; Stargardter, F. *Arch. Dermatol.* **1963**, *87*, 601.
2. Schmitz, F. J.; Vanderah, D. J.; Hollenbeak, K. H.; Enwall, C. E. L.; Gopichand, Y. *J. Org. Chem.* **1983**, *48*, 3941.
3. Dillman, R. L.; Cardellina, J. H., II *J. Nat. Prod.* **1991**, *54*, 1159.
4. Dillman, R. L.; Cardellina, J. H., II *J. Nat. Prod.* **1991**, *54*, 1056.
5. Hentschel, U.; Usher, K. M.; Taylor, M. W. *FEMS Microbiol. Ecol.* **2006**, *55*, 167.
6. Stierle, A. C.; Cardellina, J. H., II; Singleton, F. L. *Experientia* **1988**, *44*, 1021.
7. Stierle, A. A.; Cardellina, J. H., II *Tetrahedron Lett.* **1991**, *32*, 4847.
8. Schmitz, F. J.; Gunasekera, S. P.; Yalamanchili, G.; Hossain, M. B.; van der Helm, D. *J. Am. Chem. Soc.* **1984**, *106*, 7251.
9. Chen, W.; Tang, W.; Zhang, R.; Lou, L.; Zhao, W. *J. Nat. Prod.* **2007**, *70*, 567.
10. Dale, J. A.; Mosher, H. S. *J. Am. Chem. Soc.* **1993**, *95*, 512; Ohtani, I.; Kusumi, T.; Kashman, Y.; Kakisawa, H. *J. Am. Chem. Soc.* **1991**, *113*, 4092.
11. Posadas, I.; Bucci, M.; Roviezzo, F.; Rossi, A.; Parente, L.; Sautebin, L.; Cirino, G. *J. Pharmacol.* **2004**, *142*, 331.
12. Henriques, M. G.; Silva, P. M.; Martins, M. A.; Flores, C. A.; Cunha, F. Q.; Assreuy-Fiho, J.; Cordeiro, A. *Braz. J. Med. Biol. Res.* **1987**, *20*, 243–249.
13. Gonzalez, A. G.; Ciccio, J. F.; Rivera, A. P.; Martin, J. D. *J. Org. Chem.* **1985**, *50*, 1261.
14. Guella, G.; Mancini, I.; Pietra, F. *Comp. Biochem. Physiol.* **1992**, *103B*, 1019.
15. Although in Ref. 13 and in all the subsequent literature (including Ref. 14) the compound is described as an isopimarane (i.e., 13-*epi*-pimarane), the structural drawing on the paper shows the stereochemistry of a pimarane. Because the stereochemical assignment was only based on analogy with known compounds, the actual stereochemistry at C-13 of the bromoditerpene from *L. perforata* remains undetermined.
16. Kim, Y. H.; Chung, B. S.; Sankawa, U. *J. Nat. Prod.* **1988**, *51*, 1080.
17. Suh, Y. G.; Kim, Y. H.; Park, M. H.; Choi, Y. H.; Lee, H. K.; Moon, J. Y.; Min, K. H.; Shin, D. Y.; Jung, J. K.; Park, O. H.; Jeon, R. O.; Park, H. S.; Kang, S. A. *Bioorg. Med. Chem. Lett.* **2001**, *11*, 559.
18. Suh, Y. G.; Lee, K. O.; Moon, S. H.; Seo, S. Y.; Lee, Y. S.; Kim, S. H.; Paek, S. M.; Kim, Y. H.; Lee, Y. S.; Jeong, J. M.; Lee, S. J.; Kim, S. G. *Bioorg. Med. Chem. Lett.* **2004**, *14*, 3487.
19. Posadas, I.; Terencio, M. C.; Guillén, I.; Ferrándiz, M. L.; Coloma, J.; Payá, M.; Alcaraz, M. J. *Naunyn-Schmied. Arch. Pharmacol.* **2000**, *361*, 98.